

Towards Understanding the Condensation of Two-layer Neural Networks at Initial Training

Zhi-Qin John Xu^{1,*}, Hanxu Zhou^{1,†}, Tao Luo¹, Yaoyu Zhang^{1,2,‡}

¹ School of Mathematical Sciences, Institute of Natural Sciences, MOE-LSC and Qing Yuan Research Institute, Shanghai Jiao Tong University

² Shanghai Center for Brain Science and Brain-Inspired Technology

Abstract

Studying the implicit regularization effect of the nonlinear training dynamics of neural networks (NNs) is important for understanding why over-parameterized neural networks often generalize well on real dataset. Empirically, existing works have shown that weights of NNs condense on isolated orientations with a small initialization. The condensation dynamics implies that NNs can learn features from the training data with a network configuration effectively equivalent to a much smaller network during the training. In this work, we show that the multiple roots of activation function at origin is a key factor to understanding the condensation at the initial stage of training. Our experiments suggest that the maximal number of condensed orientations is twice of the multiplicity. Our theoretical analysis confirms experiments for two cases, one is for the activation function of multiplicity one and the other is for the one-dimensional input. This work makes a step towards understanding how small initialization implicitly leads NNs to condensation at initial stage of training, which lays a solid foundation for the future study of the nonlinear dynamics of NNs and its implicit regularization effect at a later stage of training.

1 Introduction

Mildly overparameterized neural networks often show good generalization performance on real-world problems by minimizing a loss function without explicit regularizations (Breiman, 1995; Zhang et al., 2017). From the perspective of approximation, for over-parameterized NNs, there are infinite possible sets of training parameters that can reach a satisfying training loss. However, their generalization performances can be very different. It is important to study what implicit regularization is imposed aside to the loss function during the training that leads the NN to a specific type of solutions.

Recent studies on the training behavior have rendered significant understanding on NNs. Empirical works suggest that NNs may learn the data from simple to complex patterns (Arpit et al., 2017; Xu et al., 2019; Rahaman et al., 2019; Xu et al., 2020; Jin et al., 2020; Kalimeris et al., 2019). For example, an implicit bias of frequency principle (or spectral bias) is widely observed that NNs often learn the target function from low to high frequency (Xu et al., 2019; Rahaman et al., 2019; Xu et al., 2020). However, frequency is a coarse-grained characterization of a function without much detail. At the initial training stage, the low-frequency function learned by the NNs can be various types, such as low-frequency sinusoidal functions or low-order polynomials. Kalimeris et al. (2019) find that the initial learning of ReLU NNs may be similar to a linear model (*linear w.r.t. the input but not*

*Co-first author and corresponding author: xuzhiqin@sjtu.edu.cn.

†Co-first author.

‡Corresponding author: zhyysjtu@sjtu.edu.cn.

parameters) by the measurement of mutual information. However, it is still not clear *how simple the NN output can be at the initial stage of learning*.

The NN output, either simple or complex, is a collective result of all neurons. The study of how neuron weights evolve during the training is central to understanding the collective behavior, including the complexity, of NN output. An infinite-width NN in the well-studied neural tangent kernel (NTK) regime or lazy training regime resembles a random feature model (Jacot et al., 2018; Arora et al., 2019; Zhang et al., 2020; Weinan et al., 2020; Chizat and Bach, 2019), which uses the features given by the initialization to learn training data. Thus, NTK analysis cannot show the superiority of NNs over random feature models. Both empirical and theoretical studies show that an infinite-width NN with the initialization in the mean-field regime (or rich regime) exhibits highly nonlinear learning dynamics (Mei et al., 2018; Rotskoff and Vanden-Eijnden, 2018; Chizat and Bach, 2018; Sirignano and Spiliopoulos, 2020). Luo et al. (2021) establish a phase diagram to study the effect of initialization for two-layer ReLU NN at the infinite-width limit and find that NTK initialization and mean-field initialization are special cases of linear regime and critical regime, respectively. Rest to the linear and the critical regime in the phase diagram is a largely unexplored non-linear regime. This non-linear regime, where parameters of a NN are initialized towards infinitesimal, is named condensed regime because the features of hidden neurons (orientations of the input weight) condense in several isolated orientations during the training (Luo et al., 2021). The condensation is a feature learning process, which is important to learning of DNNs. Note that in the following, *condensation is accompanied by a default assumption of small initialization*. The condensation transforms a large network to a network of only a few effective neurons throughout the training, leading to a simple output function. Therefore, the study of condensation could provide insight into how NNs are implicitly regularized to achieve good generalization performance in practice. For two-layer ReLU, Maennel et al. (2018) prove that, as the initialization of parameters goes to zero, the features of hidden neurons condensed at finite number of orientations depending on the input data; when performing a linearly separable classification task with infinite data, Pellegrini and Biroli (2020) show that at mean-field limit, a two-layer infinite-width ReLU NN is effectively a NN of one hidden neuron, i.e., condensation on a single orientation. Both work (Maennel et al., 2018; Pellegrini and Biroli, 2020) study the condensation behavior for ReLU-NNs at a initial training stage in which the magnitudes of NN parameters are far smaller from well-fitting an $O(1)$ target function. However, it still remains unclear that *for NNs of more general activation functions, how the condensation emerges at the initial training stage*.

In this work, we show that the condensation at the initial stage is closely related to the multiplicity p at $x = 0$, which means derivative of activation at $x = 0$ is zero up to the $(p - 1)$ th-order and is non-zero for the p -th order. For finite-width two-layer NNs with small initialization at the initial training stage, each hidden neuron’s output in a finite domain around 0 can be approximated by a p -th order polynomial and so is the NN output function. Based on the p -th order approximation, we prove that the NN at most condenses at $2p$ orientations by experiments and a preliminary theory. Therefore, small initialization imposes an implicit regularization that restricts the hypothesis function space to be low-complexity at the initial learning stage. This implicit regularization holds regardless of how overparameterized a NN is. Thus, the generalization gap of NN at initial stage of training should be small, conforming with previous empirical results (Breiman, 1995; Zhang et al., 2017). Our study of initial training behavior lays a solid ground for the further study of the dynamics and implicit regularization of NNs throughout the training.

2 Related works

Arpit et al. (2017) measure the number of critical training samples which is close to the classification boundary and find that such critical number increases as the training, thus, intuitively suggesting that the classification function may be increasingly complex during the training. Xu et al. (2019); Rahaman et al. (2019); Xu et al. (2020) utilize frequency to quantitatively find that NNs often learn the target function from low to high frequency, which is called frequency principle (or spectral bias). Frequency principle shows an implicit bias in the frequency domain during the training that qualitatively explains why NNs work well for the low-frequency dominant problems but badly for the high-frequency dominant problems Xu et al. (2020), and further inspired a series of algorithms for fast learning high frequency (Xu et al., 2020; Jagtap et al., 2020; Biland et al., 2019; Cai et al., 2020;

Peng et al., 2020; Cai and Xu, 2019; Liu et al., 2020; Li et al., 2020; Wang, 2020; Tancik et al., 2020; Mildenhall et al., 2020; Agarwal et al., 2020; Campo et al., 2020; Jiang et al., 2020; Xi et al., 2020).

Another research line studies how initialization affects the weight evolution of NNs with a sufficient large or infinite width. For example, with an initialization in neural tangent kernel (NTK) regime or lazy training regime (weights change slightly during the training), the gradient flow of infinite-width NN, can be approximated by a linear dynamics of random feature model (Jacot et al., 2018; Arora et al., 2019; Zhang et al., 2020; Weinan et al., 2020; Chizat and Bach, 2019), whereas for the initialization in the mean-field regime (weights change significantly during the training), the gradient flow of infinite-width NN exhibits highly nonlinear dynamics (Mei et al., 2019; Rotskoff and Vanden-Eijnden, 2018; Chizat and Bach, 2018; Sirignano and Spiliopoulos, 2020). Pellegrini and Biroli (2020) analyze how the dynamics of each parameter transforms from a lazy regime (NTK initialization) to a rich regime (mean-field initialization) for an two-layer infinite-width ReLU NN to perform a linearly separable classification task with infinite data. Luo et al. (2021) systematically study the effect of initialization for two-layer ReLU NN with infinite width by establishing a phase diagram, which shows three distinct regimes, i.e., *linear* regime (similar to the lazy regime), *critical* regime and *condensed* regime (similar to the rich regime), based on the relative change of input weights as the width approaches infinity, which tends to 0, $O(1)$ and $+\infty$, respectively. NTK initialization is a specific example of the linear regime, while the mean-field initialization is a specific example of the critical regime, which serves as the boundary between the other two regimes. Luo et al. (2021) also empirically finds that, in the condensed regime, the features of hidden neurons (orientation of the input weight) condense in several isolated orientations, which is a strong feature learning behavior, an important characteristic of deep learning.

3 Preliminary: Two-layer neural networks

In this work, we study the following two-layer NN

$$f_{\theta}(\mathbf{x}) = \sum_{j=1}^m a_j \sigma(\mathbf{w}_j \cdot \mathbf{x}), \quad (1)$$

where $\sigma(\cdot)$ is the activation function, $\mathbf{w}_j = (\bar{\mathbf{w}}_j, \mathbf{b}_j) \in \mathbb{R}^{d+1}$ is the neuron feature including the input weight and bias terms, and $\mathbf{x} = (\bar{\mathbf{x}}, 1) \in \mathbb{R}^{d+1}$ is combination of the input sample and scalar 1, θ is the set of all parameters. For simplicity, we call \mathbf{w}_j weight and \mathbf{x} input sample. The target function is denoted as $f^*(\mathbf{x})$. The training loss function is mean squared error

$$R_S(\theta) = \frac{1}{2n} \sum_{i=1}^n (f_{\theta}(\mathbf{x}_i) - f^*(\mathbf{x}_i))^2. \quad (2)$$

We consider the gradient flow training, by which dynamics of each neuron j is governed by

$$\dot{a}_j = -\frac{1}{n} g_{\theta}(\mathbf{w}_j), \quad \dot{\mathbf{w}}_j = -\frac{a}{n} \nabla g_{\theta}(\mathbf{w}_j),$$

where

$$g_{\theta}(\mathbf{w}) := \sum_{i=1}^n (f_{\theta}(\mathbf{x}_i) - f^*(\mathbf{x}_i)) \sigma(\mathbf{w} \cdot \mathbf{x}_i).$$

From the particle point of view, $g_{\theta}(\mathbf{w})$ serves as potential energy directing the evolution of each feature vector \mathbf{w}_j . To understand the impact of $g_{\theta}(\mathbf{w})$ given θ , our analysis focuses on the following dynamics for a test neuron at an arbitrary location (a, \mathbf{w})

$$\dot{a} = -\frac{1}{n} g_{\theta}(\mathbf{w}), \quad \dot{\mathbf{w}} = -\frac{a}{n} \nabla g_{\theta}(\mathbf{w}). \quad (3)$$

For analysis, we further define

$$r := \|\mathbf{w}\|_2, \quad \mathbf{u} := \mathbf{w} / \|\mathbf{w}\|_2, \quad (4)$$

whose evolution follows

$$\dot{r} = \mathbf{u} \cdot \dot{\mathbf{w}}, \quad \dot{\mathbf{u}} = \frac{\dot{\mathbf{w}} - (\dot{\mathbf{w}} \cdot \mathbf{u}) \mathbf{u}}{r}. \quad (5)$$

For convenience, we characterize the activation function by the following definition.

Definition 1 (multiplicity p). Suppose that $\sigma(x)$ satisfies the following condition, there exists a $p \in \mathbb{N}$ and $p \geq 1$, such that the k -th order derivative $\sigma^{(k)}(0) = 0$ for $k = 1, 2, \dots, p-1$, and $\sigma^{(p)}(0) \neq 0$, then we say σ has multiplicity p .

4 Initial condensation of input weights

It is intuitively believed that NNs are powerful at learning data features, which should be an important reason behind the success of deep learning. A simple way to define a learned feature of a neuron is by the orientation of its input weights. Previous work in Luo et al. (2021) show that there is a condensed regime, where the neuron features condense on isolated orientations during the training for two-layer ReLU NNs. The condensation implicates that although there are many more neurons than samples, the number of effective neurons, i.e., the number of different used features in fitting, is often much less than samples. Therefore, the condensation provides a potential mechanism that helps overparameterized NNs avoid overfitting (Breiman, 1995; Zhang et al., 2017). However, it is still unclear how the condensation, for general NNs with small initialization, emerges during the training. In this section, we would empirically show how the condensation differs among NNs with activation functions of different multiplicity, followed by theoretical analysis in the next section.

We consider the evolution of the features in two-layer NN in (5), i.e., the director of the input weight, defined by $\mathbf{u} = \mathbf{w} / \|\mathbf{w}\|_2$. Here, we use “director” instead of “orientation” in order not to distinguish the two directions of a line, i.e. \mathbf{n} and $-\mathbf{n}$ are equivalent. In (5) the direction of \mathbf{u} depends on the sign of a . Without distinguishing the two opposite directions, we can ignore the effect of a but focus on the evolution of \mathbf{u} .

4.1 High-dimensional data

We first show the condensation at initial training stage in fitting high-dimensional data set. Since the input is a high-dimensional vector, the director is also high-dimensional. To characterize the condensation, we define the distance (denoted by $D(\mathbf{u}, \mathbf{v})$) between the two directors (unit vectors of input weights, denoted by \mathbf{u}, \mathbf{v}) by their inner product,

$$D(\mathbf{u}, \mathbf{v}) = \mathbf{u}^\top \mathbf{v}. \quad (6)$$

The 80 training data in the experiment in Fig. 1 are sampled from a 5-dimensional function $\sum_{k=1}^5 3.5x_k \sin(5x_k + 1)$, where $\mathbf{x} = (x_1, x_2, \dots, x_5)^\top \in \mathbb{R}^5$. As shown in Fig. 1(a), the NN with activation function $\tanh(x)$ condensed at two opposite directions, i.e., one line. As the multiplicity increasing, NNs with $x \tanh(x)$ (Fig. 1(b)) and $x^2 \tanh x$ (Fig. 1(c)) condensed at two and three different lines, respectively. For ReLU, for which the multiplicity definition cannot apply, in Fig. 1(d), the NN condenses at three directions, in which two are opposite. Therefore, the multiplicity of the activation function may underlie the condensation complexity at initial training.

Note that if the target function is simpler, directors may condense at fewer directions. For example, as shown in Fig. 2(a), compared with the high frequency function in Fig. 1, we only change the target function to be a simpler function, i.e., $\sum_{k=1}^5 3.5x_k \sin(x_k + 1)$, the NN with $x^2 \tanh(x)$ only condenses at two lines. For MNIST data⁴ in Fig. 2(b), we find that, the NN with $x^2 \tanh(x)$ condenses at one line, which may suggest that MNIST dataset is a simple dataset.

To understand the mechanism of the initial condensation, we turn to 1-dimensional experiments, which can be clearly visualized in the next subsection.

4.2 1-dimensional data

For 1-dimensional data, we can visualize the evolution of the NN output and each weight, which would further confirm the connection between the condensation and the multiplicity of the activation function.

The experiments are set up as follows. The training data is 40 points sampled from $\sin(3x) + \sin(6x)/2$, illustrated by green dots in Fig. 3. We train a two-layer NN of 100 hidden neurons with

⁴<http://yann.lecun.com/exdb/mnist/>

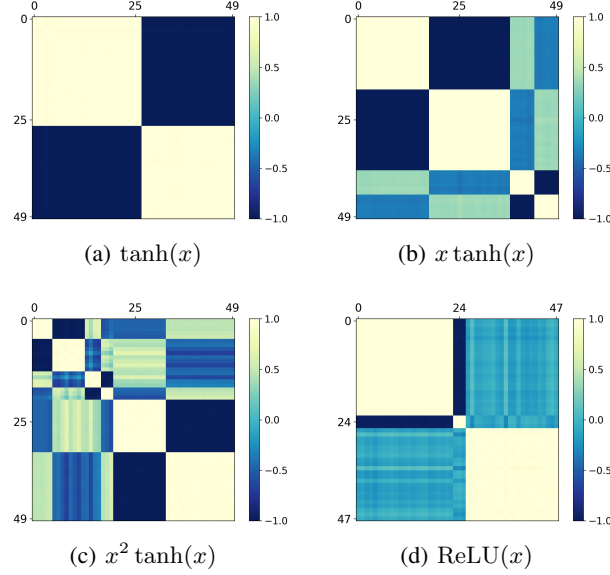


Figure 1: Weight condensation of NNs with different activation functions indicated by the sub-captions. The color of the 50×50 matrix indicates the inner product of every two corresponding normalized input weights from all 50 weights, except for sub-figure (d). In sub-figure (d), as we discard the input weight with very small amplitude, the matrix is 48×48 . If the inner product of two normalized input weights is close to 1 or -1, then they are almost on a line. The training data is 80 points sampled from a 5-dimensional function $\sum_{k=1}^5 3.5x_k \sin(5x_k + 1)$. The NN with 50 hidden neurons is initialized by a Gaussian function $N(0, 0.005)$ and trained with MSE loss and Adam optimizer.

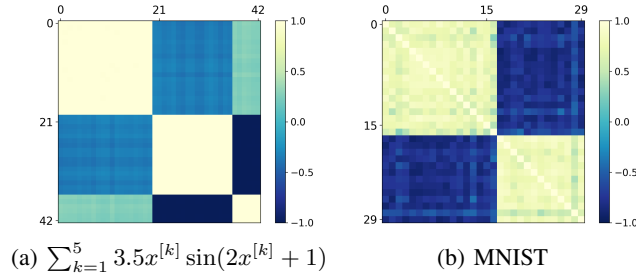


Figure 2: Weight condensation of NN with activation function $x^2 \tanh(x)$. All setting in the sub-figure (a) is the same as Fig. 1, except for the target function $\sum_{k=1}^5 3.5x^{[k]} \sin(2x^{[k]} + 1)$. Similarly, we discard the input weight with very small amplitude, leading the matrix to 42×42 . The training data in the sub-figure (b) is the MNIST data-set. The NN with 30 hidden neurons is initialized by a Gaussian function $N(0, 0.001)$ and trained with MSE loss and Adam optimizer in the sub-figure (b).

Adam optimizer, full batch, learning rate 0.0005, and mean squared error loss. All parameters are initialized by samples following Gaussian distribution $N(0, 0.005)$.

We display the output at initial training, epoch 1000, for NNs with activation function $\tanh(x)$, $x \tanh(x)$, $x^2 \tanh(x)$, and $\text{ReLU}(x)$ in Fig. 3. Due to the small values of parameters, an activation function with multiplicity p can be well approximated by a p -th order polynomial, thus, the NN output can also be approximated by a p -th order polynomial. As shown in Fig. 3(a-c), the NN output with activation function $\tanh(x)$, $x \tanh(x)$ and $x^2 \tanh(x)$ overlaps well with the auxiliary of linear, quadratic and cubic polynomial curve, respectively. In Fig. 3(d), the NN output with ReLU activation function deviates from a linear function (red auxiliary line). Particularly, the NN output has several sharp turning points.

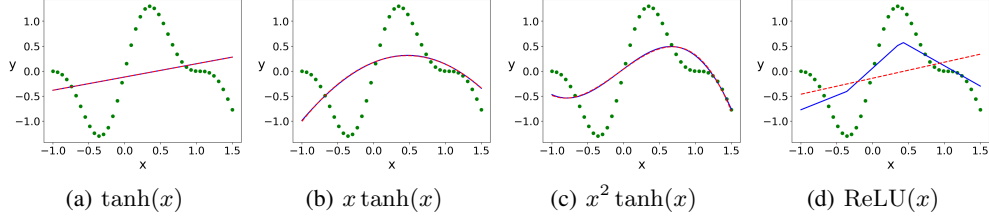


Figure 3: The outputs of NNs at training step 1000 with activation function $\tanh(x)$, $x \tanh(x)$, $x^2 \tanh(x)$, and $\text{ReLU}(x)$ are displayed, respectively. The green dots are training data, the blue solid line is the NN output at test points, the red dashed auxiliary line is the first, second, third and first order polynomial fitting of the test points for (a, b, c, d), respectively.

This experiment, although simple, but convincingly shows that NN does not always learn a linear function at the initial training stage and the complexity of such learning depends on the activation function.

We then visualize the direction field for input weight $\mathbf{w} := (w, b)$ of the dynamics in (5) in Fig. 4 with the fixed θ at different training steps. Note that, in (5), \mathbf{w} and a are independent with θ , therefore, the dynamics can be understood as the direction field of a test neuron, and by implementing an interested neuron's value to the test neuron, we can obtain the interested neuron's velocity. Since the direction of \mathbf{w} depends on the sign of a , we set $a \equiv 1$. Therefore, we are only interested in the line to which the director of \mathbf{u} is parallel. Around the original point, the field has one, two, three stables lines, on which a neuron would keep its director, for $\tanh(x)$, $x \tanh(x)$, and $x^2 \tanh(x)$, respectively. We also display the weight of each neuron at the corresponding training step on the field by the green dots and their velocity direction by the orange arrows. Similarly to the high-dimensional case, NN with multiplicity p activation function condenses at p different lines for $p = 1, 2, 3$.

As shown in the fourth row in Fig. 4, the field and the condensation for NN with $\text{ReLU}(x)$ is much more complex.

Taken together, we have empirically show that the multiplicity of the activation function is a key factor that determines the complexity of the initial output and initial condensation.

5 Analysis of the initial condensation of input weights

In this section, we would present a preliminary analysis to understand how the multiplicity of the activation function affects the initial condensation.

Suppose the activation function satisfies the multiplicity p , i.e., $\sigma^{(k)}(0) = 0$ for $k = 1, 2, \dots, p-1$, and $\sigma^{(p)}(0) \neq 0$. For convenience, we define $e_i := f_\theta(\mathbf{x}_i) - f^*(\mathbf{x}_i)$, an operator \mathcal{P} satisfying

$$\mathcal{P}\mathbf{w} := \dot{\mathbf{w}} - \mathbf{u}(\dot{\mathbf{w}} \cdot \mathbf{u}),$$

where $\mathbf{u} := \mathbf{w}/\|\mathbf{w}\|_2$. Condensation refers to that the weight evolves following dynamics (5) towards a direction that will not change in the direction field and is defined as follows,

$$\dot{\mathbf{u}} = 0 \Leftrightarrow \mathcal{P}\mathbf{w} := \dot{\mathbf{w}} - \mathbf{u}(\dot{\mathbf{w}} \cdot \mathbf{u}) = 0.$$

Since $\dot{\mathbf{w}} \cdot \mathbf{u}$ is a scalar, $\dot{\mathbf{w}}$ is parallel with \mathbf{u} . \mathbf{u} is a unit vector, therefore, we have

$$\mathbf{u} = \dot{\mathbf{w}}/\|\dot{\mathbf{w}}\|_2$$

In this work, we consider NNs with sufficiently small parameters. For small $r = \|\mathbf{w}\|_2$, dynamics (5) shows that \mathbf{u} would moves quickly to its stable direction. In the following, we study the case of (i) $p = 1$ and (ii) $d = 1$. We left other situations for future study.

5.1 Case 1: $p = 1$

Consider $\sigma'(0) \neq 0$, $e_i = f_\theta(\mathbf{x}_i) - f^*(\mathbf{x}_i)$ fixed and $\mathbf{w} = o(1)$. By Taylor expansion,

$$\mathcal{P}\mathbf{w} \stackrel{\text{leading order}}{\approx} \mathcal{Q}\mathbf{w} := -\frac{a}{n} \sum_{i=1}^n \sigma'(0) e_i \mathbf{x}_i + \left(\frac{a}{n} \sum_{i=1}^n \sigma'(0) e_i \mathbf{x}_i \cdot \mathbf{u}\right) \mathbf{u} = 0.$$

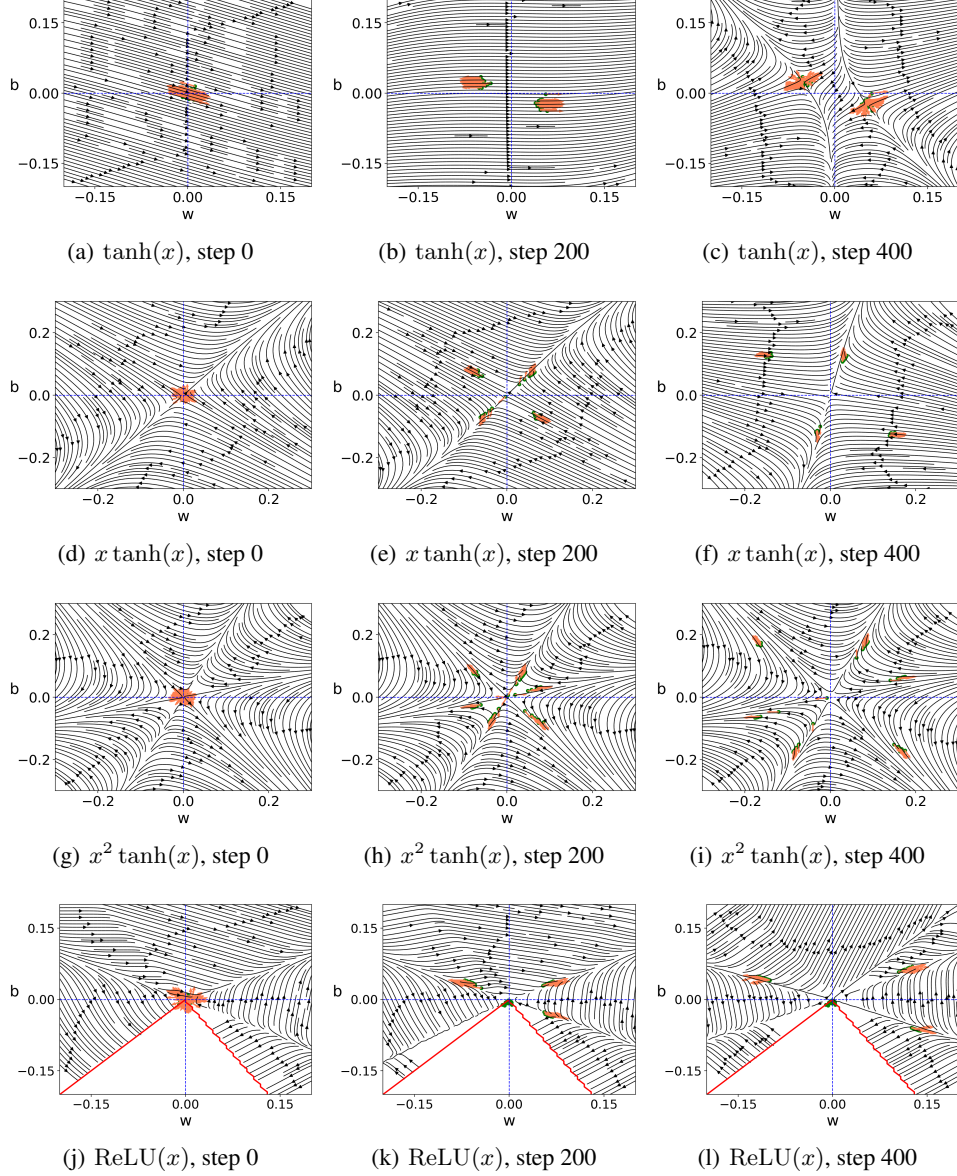


Figure 4: The direction field for input weight $\mathbf{w} := (w, b)$ of the dynamics in (5) with fixed θ at different training steps. We also display the value of each weight at the corresponding training step by the green dots and the direction by the orange arrow.

WLOG, we assume $a \neq 0$, then

$$Q\mathbf{w} = 0 \Leftrightarrow \sum_{i=1}^n e_i \mathbf{x}_i = \sum_{i=1}^n e_i (\mathbf{x}_i \cdot \mathbf{u}) \mathbf{u}.$$

We have

$$\mathbf{u} = \frac{\sum_{i=1}^n e_i \mathbf{x}_i}{\|\sum_{i=1}^n e_i \mathbf{x}_i\|_2}.$$

This indicates that there is only one solution for $Q\mathbf{w} = 0$, which only depends on the training data. Therefore, when parameters are sufficiently small, all input weights would converge to the same direction or the opposite direction, i.e., condensation on a line.

5.2 Case 2: $p > 1, d = 1$

By the definition of the multiplicity p , we have

$$\sigma'(\mathbf{w} \cdot \mathbf{x}_i) = \frac{\sigma^{(p)}(0)}{(p-1)!} (\mathbf{w} \cdot \mathbf{x}_i)^{p-1} + o((\mathbf{w} \cdot \mathbf{x}_i)^{p-1}).$$

Then up to the leading order in terms of the size of θ , we have

$$\mathcal{P}\mathbf{w} \stackrel{\text{leading order}}{\approx} \mathcal{Q}\mathbf{w} := -\frac{a}{n} \sum_{i=1}^n \frac{\sigma^{(p)}(0)}{(p-1)!} (\mathbf{w} \cdot \mathbf{x}_i)^{p-1} e_i \mathbf{x}_i + \left(\frac{a}{n} \sum_{i=1}^n \frac{\sigma^{(p)}(0)}{(p-1)!} (\mathbf{w} \cdot \mathbf{x}_i)^{p-1} e_i \mathbf{x}_i \cdot \mathbf{u} \right) \mathbf{u}.$$

Without loss of generality, we also assume $a \neq 0$, then, we have

$$\mathcal{Q}\mathbf{w} = 0 \Leftrightarrow \mathbf{u} = \frac{\sum_{i=1}^n (\mathbf{w} \cdot \mathbf{x}_i)^{p-1} e_i \mathbf{x}_i}{\left\| \sum_{i=1}^n (\mathbf{w} \cdot \mathbf{x}_i)^{p-1} e_i \mathbf{x}_i \right\|_2}.$$

Inner product with \mathbf{u} for both hand sides, we have

$$\sum_{i=1}^n (\mathbf{u} \cdot \mathbf{x}_i)^p e_i = \|\mathbf{u}\|_2^2 \left\| \sum_{i=1}^n (\mathbf{u} \cdot \mathbf{x}_i)^{p-1} e_i \mathbf{x}_i \right\|_2.$$

Since $d+1=2$, we denote $\mathbf{u} = (u_1, u_2)^\top \in \mathbb{R}^2$ and $\mathbf{x}_i = ((\mathbf{x}_i)_1, (\mathbf{x}_i)_2)^\top \in \mathbb{R}^2$, then,

$$\frac{\sum_{i=1}^n (u_1(\mathbf{x}_i)_1 + u_2(\mathbf{x}_i)_2)^{p-1} e_i (\mathbf{x}_i)_1}{\sum_{i=1}^n (u_1(\mathbf{x}_i)_1 + u_2(\mathbf{x}_i)_2)^{p-1} e_i (\mathbf{x}_i)_2} = \frac{u_1}{u_2} \triangleq \hat{u}.$$

We obtain the equation for \hat{u} ,

$$\sum_{i=1}^n (\hat{u}(\mathbf{x}_i)_1 + (\mathbf{x}_i)_2)^{p-1} e_i (\mathbf{x}_i)_1 = \hat{u} \sum_{i=1}^n (\hat{u}(\mathbf{x}_i)_1 + (\mathbf{x}_i)_2)^{p-1} e_i (\mathbf{x}_i)_2.$$

Since it is an univariate p -th order equation, $\hat{u} = \frac{u_1}{u_2}$ has at most p complex roots. Because \mathbf{u} is a unit vector, \mathbf{u} at most has p pairs of values, in which each pair are opposite.

Taken together, our preliminary theoretical analysis is consistent with our experiments, that is, the multiplicity of activation function at $x = 0$ may underlie the number of directors the NN would condense on when parameters are infinitesimal.

6 Discussion

In this work, we have shown that the characteristic of the activation function, i.e., multiplicity, is a key factor to understanding the complexity of NN output and the weight condensation at initial training. The condensation restricts the NN to be effectively low-capacity at the initial training stage, even for finite-width NNs. During the training, the NN increases its capacity to better fit the data, leading to a potential explanation for their good generalization in practical problems. This work also serves as a starting point for further studying the condensation for multiple-layer neural networks throughout the training process.

How small the initialization should be in order to see a clear condensation is studied in Luo et al. (2021) for two-layer ReLU NNs with infinite width. For general activation functions, the regime of the initialization for condensation depends on the NN width. A further study of the phase diagram for finite width NNs would be important.

For general multiplicity with high-dimensional input data, the theoretical analysis for the initial condensation is a very difficult problem, which is equivalent to count the number of the roots of a high-order high-dimensional polynomial with a special structure originated from NNs.

Acknowledgments and Disclosure of Funding

This work is sponsored by the National Key R&D Program of China Grant No. 2019YFA0709503 (Z. X.), the Shanghai Sailing Program, the Natural Science Foundation of Shanghai Grant No.

20ZR1429000 (Z. X.), the National Natural Science Foundation of China Grant No. 62002221 (Z. X.), Shanghai Municipal of Science and Technology Project Grant No. 20JC1419500 (Y.Z.), Shanghai Municipal of Science and Technology Major Project No. 2021SHZDZX0102, and the HPC of School of Mathematical Sciences and the Student Innovation Center at Shanghai Jiao Tong University.

References

- L. Breiman, Reflections after refereeing papers for nips, *The Mathematics of Generalization XX* (1995) 11–15.
- C. Zhang, S. Bengio, M. Hardt, B. Recht, O. Vinyals, Understanding deep learning requires rethinking generalization, in: *5th International Conference on Learning Representations, ICLR 2017, Toulon, France, April 24-26, 2017, Conference Track Proceedings, OpenReview.net, 2017*. URL: <https://openreview.net/forum?id=Sy8gdB9xx>.
- D. Arpit, S. Jastrzebski, N. Ballas, D. Krueger, E. Bengio, M. S. Kanwal, T. Maharaj, A. Fischer, A. C. Courville, Y. Bengio, S. Lacoste-Julien, A closer look at memorization in deep networks, in: D. Precup, Y. W. Teh (Eds.), *Proceedings of the 34th International Conference on Machine Learning, ICML 2017, Sydney, NSW, Australia, 6-11 August 2017, volume 70 of Proceedings of Machine Learning Research, PMLR, 2017*, pp. 233–242. URL: <http://proceedings.mlr.press/v70/arpit17a.html>.
- Z.-Q. J. Xu, Y. Zhang, Y. Xiao, Training behavior of deep neural network in frequency domain, *International Conference on Neural Information Processing* (2019) 264–274.
- N. Rahaman, D. Arpit, A. Baratin, F. Draxler, M. Lin, F. A. Hamprecht, Y. Bengio, A. Courville, On the spectral bias of deep neural networks, *International Conference on Machine Learning* (2019).
- Z.-Q. J. Xu, Y. Zhang, T. Luo, Y. Xiao, Z. Ma, Frequency principle: Fourier analysis sheds light on deep neural networks, *Communications in Computational Physics* 28 (2020) 1746–1767.
- P. Jin, L. Lu, Y. Tang, G. E. Karniadakis, Quantifying the generalization error in deep learning in terms of data distribution and neural network smoothness, *Neural Networks* 130 (2020) 85–99.
- D. Kalimeris, G. Kaplun, P. Nakkiran, B. L. Edelman, T. Yang, B. Barak, H. Zhang, SGD on neural networks learns functions of increasing complexity, in: H. M. Wallach, H. Larochelle, A. Beygelzimer, F. d’Alché-Buc, E. B. Fox, R. Garnett (Eds.), *Advances in Neural Information Processing Systems 32: Annual Conference on Neural Information Processing Systems 2019, NeurIPS 2019, December 8-14, 2019, Vancouver, BC, Canada, 2019*, pp. 3491–3501. URL: <https://proceedings.neurips.cc/paper/2019/hash/b432f34c5a997c8e7c806a895ecc5e25-Abstract.html>.
- A. Jacot, C. Hongler, F. Gabriel, Neural tangent kernel: Convergence and generalization in neural networks, in: S. Bengio, H. M. Wallach, H. Larochelle, K. Grauman, N. Cesa-Bianchi, R. Garnett (Eds.), *Advances in Neural Information Processing Systems 31: Annual Conference on Neural Information Processing Systems 2018, NeurIPS 2018, December 3-8, 2018, Montréal, Canada, 2018*, pp. 8580–8589. URL: <https://proceedings.neurips.cc/paper/2018/hash/5a4belfa34e62bb8a6ec6b91d2462f5a-Abstract.html>.
- S. Arora, S. S. Du, W. Hu, Z. Li, R. Salakhutdinov, R. Wang, On exact computation with an infinitely wide neural net, in: H. M. Wallach, H. Larochelle, A. Beygelzimer, F. d’Alché-Buc, E. B. Fox, R. Garnett (Eds.), *Advances in Neural Information Processing Systems 32: Annual Conference on Neural Information Processing Systems 2019, NeurIPS 2019, December 8-14, 2019, Vancouver, BC, Canada, 2019*, pp. 8139–8148. URL: <https://proceedings.neurips.cc/paper/2019/hash/dbc4d84bfcfe2284ballbeffb853a8c4-Abstract.html>.
- Y. Zhang, Z.-Q. J. Xu, T. Luo, Z. Ma, A type of generalization error induced by initialization in deep neural networks, in: *Mathematical and Scientific Machine Learning, PMLR, 2020*, pp. 144–164.
- E. Weinan, C. Ma, L. Wu, A comparative analysis of optimization and generalization properties of two-layer neural network and random feature models under gradient descent dynamics, *Science China Mathematics* (2020) 1–24.

- L. Chizat, F. Bach, A note on lazy training in supervised differentiable programming, in: 32nd Conf. Neural Information Processing Systems (NeurIPS 2018), 2019.
- S. Mei, A. Montanari, P.-M. Nguyen, A mean field view of the landscape of two-layer neural networks, *Proceedings of the National Academy of Sciences* 115 (2018) E7665–E7671.
- G. M. Rotskoff, E. Vanden-Eijnden, Parameters as interacting particles: long time convergence and asymptotic error scaling of neural networks, in: S. Bengio, H. M. Wallach, H. Larochelle, K. Grauman, N. Cesa-Bianchi, R. Garnett (Eds.), *Advances in Neural Information Processing Systems 31: Annual Conference on Neural Information Processing Systems 2018, NeurIPS 2018, December 3-8, 2018, Montréal, Canada, 2018*, pp. 7146–7155. URL: <https://proceedings.neurips.cc/paper/2018/hash/196f5641aa9dc87067da4ff90fd81e7b-Abstract.html>.
- L. Chizat, F. Bach, On the global convergence of gradient descent for over-parameterized models using optimal transport, in: *Proceedings of the 32nd International Conference on Neural Information Processing Systems*, 2018, pp. 3040–3050.
- J. Sirignano, K. Spiliopoulos, Mean field analysis of neural networks: A central limit theorem, *Stochastic Processes and their Applications* 130 (2020) 1820–1852.
- T. Luo, Z.-Q. J. Xu, Z. Ma, Y. Zhang, Phase diagram for two-layer relu neural networks at infinite-width limit, *Journal of Machine Learning Research* 22 (2021) 1–47.
- H. Maennel, O. Bousquet, S. Gelly, Gradient descent quantizes relu network features, *arXiv preprint arXiv:1803.08367* (2018).
- F. Pellegrini, G. Biroli, An analytic theory of shallow networks dynamics for hinge loss classification, *Advances in Neural Information Processing Systems* 33 (2020).
- A. D. Jagtap, K. Kawaguchi, G. E. Karniadakis, Adaptive activation functions accelerate convergence in deep and physics-informed neural networks, *Journal of Computational Physics* 404 (2020) 109136.
- S. Biland, V. C. Azevedo, B. Kim, B. Solenthaler, Frequency-aware reconstruction of fluid simulations with generative networks, *arXiv preprint arXiv:1912.08776* (2019).
- W. Cai, X. Li, L. Liu, A phase shift deep neural network for high frequency approximation and wave problems, *SIAM Journal on Scientific Computing* 42 (2020) A3285–A3312.
- W. Peng, W. Zhou, J. Zhang, W. Yao, Accelerating physics-informed neural network training with prior dictionaries, *arXiv preprint arXiv:2004.08151* (2020).
- W. Cai, Z.-Q. J. Xu, Multi-scale deep neural networks for solving high dimensional pdes, *arXiv preprint arXiv:1910.11710* (2019).
- Z. Liu, W. Cai, Z.-Q. J. Xu, Multi-scale deep neural network (mscalednn) for solving poisson-boltzmann equation in complex domains, *Communications in Computational Physics* 28 (2020) 1970–2001.
- X.-A. Li, Z.-Q. J. Xu, L. Zhang, A multi-scale dnn algorithm for nonlinear elliptic equations with multiple scales, *Communications in Computational Physics* 28 (2020) 1886–1906.
- B. Wang, Multi-scale deep neural network (mscalednn) methods for oscillatory stokes flows in complex domains, *Communications in Computational Physics* 28 (2020) 2139–2157.
- M. Tancik, P. P. Srinivasan, B. Mildenhall, S. Fridovich-Keil, N. Raghavan, U. Singhal, R. Ramamoorthi, J. T. Barron, R. Ng, Fourier features let networks learn high frequency functions in low dimensional domains, *arXiv preprint arXiv:2006.10739* (2020).
- B. Mildenhall, P. P. Srinivasan, M. Tancik, J. T. Barron, R. Ramamoorthi, R. Ng, Nerf: Representing scenes as neural radiance fields for view synthesis, in: *European Conference on Computer Vision*, Springer, 2020, pp. 405–421.

- R. Agarwal, N. Frosst, X. Zhang, R. Caruana, G. E. Hinton, Neural additive models: Interpretable machine learning with neural nets, arXiv preprint arXiv:2004.13912 (2020).
- M. Campo, Z. Chen, L. Kung, K. Virochsiri, J. Wang, Band-limited soft actor critic model, arXiv preprint arXiv:2006.11431 (2020).
- L. Jiang, B. Dai, W. Wu, C. C. Loy, Focal frequency loss for generative models, arXiv preprint arXiv:2012.12821 (2020).
- Y. Xi, W. Jia, J. Zheng, X. Fan, Y. Xie, J. Ren, X. He, Drl-gan: Dual-stream representation learning gan for low-resolution image classification in uav applications, IEEE Journal of selected topics in applied earth observations and remote sensing (2020).
- S. Mei, T. Misiakiewicz, A. Montanari, Mean-field theory of two-layers neural networks: dimension-free bounds and kernel limit, in: A. Beygelzimer, D. Hsu (Eds.), Conference on Learning Theory, COLT 2019, 25-28 June 2019, Phoenix, AZ, USA, volume 99 of *Proceedings of Machine Learning Research*, PMLR, 2019, pp. 2388–2464. URL: <http://proceedings.mlr.press/v99/mei19a.html>.

Checklist

1. For all authors...
 - (a) Do the main claims made in the abstract and introduction accurately reflect the paper’s contributions and scope? [Yes]
 - (b) Did you describe the limitations of your work? [Yes] See Section 6.
 - (c) Did you discuss any potential negative societal impacts of your work? [N/A]
 - (d) Have you read the ethics review guidelines and ensured that your paper conforms to them? [Yes]
2. If you are including theoretical results...
 - (a) Did you state the full set of assumptions of all theoretical results? [Yes] See Section 5.
 - (b) Did you include complete proofs of all theoretical results? [Yes] See Section 5.
3. If you ran experiments...
 - (a) Did you include the code, data, and instructions needed to reproduce the main experimental results (either in the supplemental material or as a URL)? [Yes] In the material.
 - (b) Did you specify all the training details (e.g., data splits, hyperparameters, how they were chosen)? [Yes] See Section 4
 - (c) Did you report error bars (e.g., with respect to the random seed after running experiments multiple times)? [N/A]
 - (d) Did you include the total amount of compute and the type of resources used (e.g., type of GPUs, internal cluster, or cloud provider)? [Yes] the provider information Will be shown in Acknowledgement.
4. If you are using existing assets (e.g., code, data, models) or curating/releasing new assets...
 - (a) If your work uses existing assets, did you cite the creators? [Yes] See Section 4.1 for MNIST dataset.
 - (b) Did you mention the license of the assets? [No] The MNIST dataset is well known.
 - (c) Did you include any new assets either in the supplemental material or as a URL? [No]
 - (d) Did you discuss whether and how consent was obtained from people whose data you’re using/curating? [N/A]
 - (e) Did you discuss whether the data you are using/curating contains personally identifiable information or offensive content? [N/A]
5. If you used crowdsourcing or conducted research with human subjects...
 - (a) Did you include the full text of instructions given to participants and screenshots, if applicable? [N/A]

- (b) Did you describe any potential participant risks, with links to Institutional Review Board (IRB) approvals, if applicable? [N/A]
- (c) Did you include the estimated hourly wage paid to participants and the total amount spent on participant compensation? [N/A]